Presented at the IEEE/ION Position, Location and Navigation Symposium (PLANS) 2008, in Monterey, California, May 6-8, 2008

Flight Test Results of Loose Integration of Dual Airborne Laser Scanners (DALS)/INS

Ananth K. Vadlamani, and Maarten Uijt de Haag, *Ohio University*

BIOGRAPHIES

Ananth Vadlamani is a research associate with the Avionics Engineering Center at Ohio University, Athens and is currently a Ph.D. candidate in the School of Electrical Engineering and Computer Science. He earned an M.S.E.E degree from Ohio University in 2004. His current research is focused on airborne laser scanner based range-image navigation, multi-sensor fusion and GPS/INS integrated systems.

Maarten Uijt de Haag is an Associate Professor of Electrical Engineering at Ohio University and a Principal Investigator with the Ohio University Avionics Engineering Center. He earned his Ph.D. from Ohio University and holds a B.S.E.E. and M.S.E.E. from Delft University of Technology, located in the Netherlands. He has been involved with GPS landing systems' research, advanced signal processing techniques for GPS receivers, GPS/INS integrated systems, and terrain-referenced navigation systems. The latter includes the development of terrain data base integrity monitors and laser-based navigation systems.

ABSTRACT

Aircraft positioning and navigation capability much be robust to ensure continuity of operation. Such navigation information is largely provided by an inertial navigation system (INS), which is a self-contained autonomous system. INS is usually integrated with GPS measurements to improve its accuracy and a GPS/INS package is a common feature of most navigation systems. However, these systems suffer degraded performance in non-GPS environments; such as when GPS is denied due to interference or jamming, or when GPS is unavailable as in Lunar or Martian scenarios. In recent years, the challenge of navigating in non-GPS environments has generated much interest. With this same objective, we investigate the use of dual airborne laser scanners (DALS), integrated with an INS for navigation in non-GPS and unknown terrain environments. In this paper, we present a proof-of-concept demonstration of the DALS/INS autonomous navigation system with flight-test data, collected onboard Ohio University's DC-3 aircraft over Athens, OH.

1. INTRODUCTION

The oldest form of navigation, dead-reckoning, is relevant even today in the form of inertial navigation systems (INS). INS is an autonomous (self-contained) sensor package that consists of a set of three accelerometers and three gyroscopes; the measurements of which are integrated, providing vehicle position, velocity and attitude (tilt and heading) information at high rates. However due to successive integrations of the measurements, the vehicle states of position, velocity and attitude have errors that drift over time. For this reason, the INS is usually integrated with others sensors or systems to constrain its drift error.

The integrated use of GPS/INS forms a good candidate solution to provide precise navigational capability and many forms and flavors of GPS/INS integration have been researched for a variety of applications. However, GPS signals are susceptible to unintentional interference caused by atmospheric effects, signal blockages from buildings, interference from communication equipment, as well as intentional jamming [1] that limit the use of GPS/INS integrated systems in such environments. Prior to GPS, many terrain referenced navigation (TRN) techniques were successfully employed in the past to constrain the INS error growth [2][3]. With the advancement in ranging sensor technology and computer processing power, TRN may once again be a candidate solution as an alternative means of navigation. The use of an airborne laser scanner (ALS) for TRN to provide aircraft precision approach guidance was investigated in [4]. TRN techniques are, however, operationally limited by the availability of an on-board terrain database at the location of interest. To overcome this limitation and to design a navigation system that can be operated in unknown terrain environments as well, the architecture proposed and tested in this paper, is an in-flight terrain mapping and navigation system.

The system concept, certain algorithmic aspects and simulation results of this proposed method have previously been published in [5]-[7]. For an in-depth understanding, the reader is referred to these previous works. This paper describes results obtained from flight

test data, as well as possible solutions to challenges encountered while working with real data. The proposed method is a dead-reckoning TRN technique that uses aircraft autonomous sensors, namely, two airborne laser scanners (Dual ALS or DALS), the inertial navigation system (INS) and a timing reference. The system has the potential to provide precise navigational capability to uninhabited or inhabited aerial vehicles in GPS-devoid and unknown terrain environments. The paper is organized as follows: section 2 provides a general overview of the system and section 3 briefly lists the ALS measurement processing equations and the navigation update algorithm. Section 4 describes the flight test, hardware and software setup. Section 5 covers the challenges of proper data processing, and post-processing results using the flight test data are provided in section 6, followed by conclusions and closing remarks.

2. SYSTEM DESCRIPTION

The proposed DALS/INS integrated system is a dead-reckoning TRN technique that keeps an estimate of the INS drifts using range (and pointing) information from two 2D ALS. The algorithm computes the INS drift terms which can be subtracted from the INS-computed aircraft parameters of velocity and position, thus effectively estimating the vehicle's velocity and position with respect to the environment. Attitude estimates are provided by the navigation-grade INS. The architecture uses two ALS; one pointing forward and the other one pointing either aft or downward the aerial vehicle. The fore-pointing ALS uses INS position and attitude and generates an estimated terrain model referred to as the reference environment model. The downward-pointing ALS will then illuminate and measure a major part of that same area some time later and generate a terrain model also. Both terrain model estimates are then correlated to estimate systematic INS errors such as INS drifts. The system concept is illustrated in Fig. 1. The fore and aft ALS terrain maps of fig. 1 are synthesized from a bare-earth terrain database, as used in [5]. The system block diagram is shown in Fig. 2.

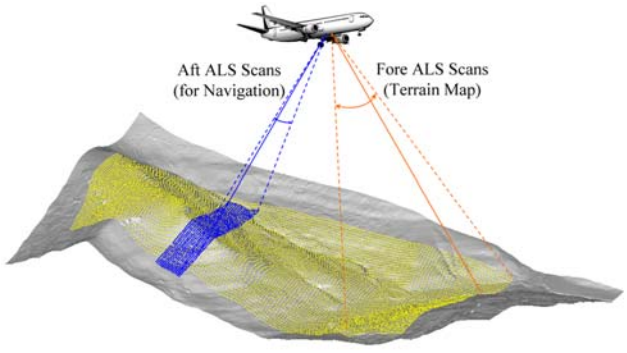

Figure 1. Dual ALS aiding concept.

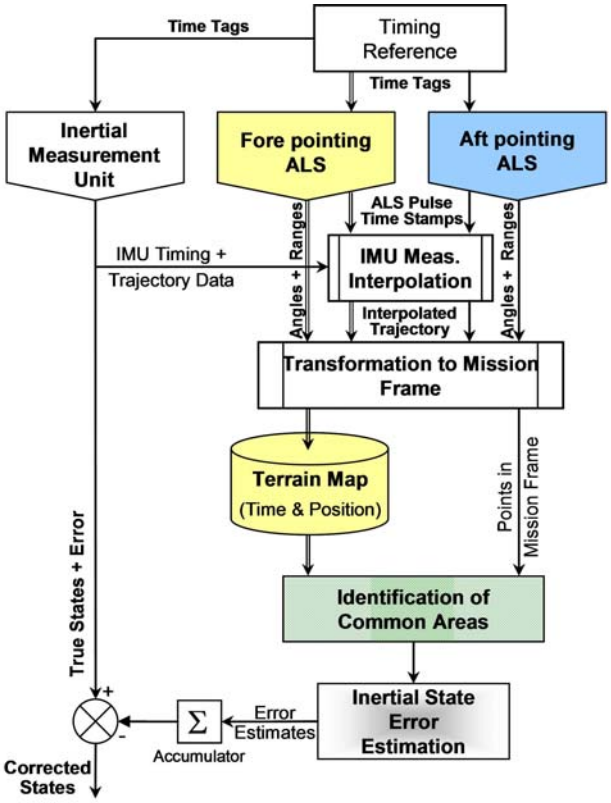

Figure 2. Block diagram of DALS aided inertial.

3. NAVIGATION FRAME PROCESSING OF ALS MEASUREMENTS

In this section, we provide mathematical expressions for the processing blocks of Fig. 2. In addition, a brief description of the complete algorithm is reproduced from [7] for completeness. The pulse repetition frequencies (PRF) of both ALS sensors far exceed the INS update rate and hence the INS values (position, attitude) are interpolated at each of the laser time-stamps. This INS interpolation process compensates for aircraft motion and the ALS pulse footprint coordinates can be a true representation of the terrain. However, due to drifts present on the INS values, the ALS maps will also contain those errors which can be estimated using the DALS aiding algorithm. The algorithm can be divided into three main parts, described briefly in the following sub-sections. For a detailed treatment, the reader is referred to [5] and [6].

3.1 GEO-REFERENCING OF AIRBORNE LASER FOOTPRINTS

Geo-referencing is the process of expressing the airborne laser footprints in unambiguous, Earth-referenced, coordinates. Since drifting INS position estimates are used here, the geo-referenced WGS84 defined Earth-Centered-Earth-Fixed (ECEF) coordinates will have errors (bias + drift). Assuming that the INS drift error is

small within the map accumulation time interval (1-3 seconds, the bias error is corrected later on in the algorithm using map correlation. If the drift error is significant, contrary to our assumption, the ALS maps will be skewed and stretched. The geo-referencing procedure can be expressed using Direction Cosine Matrices (DCM) [8] and vector addition as:

$$\underline{\chi_i}^{AL} = C_{p_i}^{AL}(p\phi_i, p\theta_i, 0)\cdot[0 \quad 0 \quad r_i]^{\mathrm{T}} \tag{1}$$

$$\underline{\chi_i}^{b} = \underline{L}_{INS\to AL}^{b} + C_{AL}^{b}(d\phi, d\theta, d\psi)\cdot \underline{\chi_i}^{AL} \tag{2}$$

$$\underline{X_i}^{e} = \underline{X_i}_{craft}^{e} + C_n^e(L_i, \lambda_i, 0)\cdot C_b^n(\phi_i, \theta_i, \psi_i)\cdot \underline{\chi_i}^{b} \tag{3}$$

where,

r_i is the range measurement from the i^{th} ALS pulse,

$\underline{\chi_i}^{F}$ is the notation denoting the i^{th} laser footprint coordinate vector in the 'F' frame. The different frames are the airborne laser (AL) frame, IMU body (b) frame, a local-level North-East-Down (n) frame and the ECEF (e) frame.

$\underline{L}_{INS\to AL}^{b}$ is the lever-arm vector from the INS to the AL aperture, expressed in body frame coordinates,

$C_X^Y(\alpha, \beta, \gamma)$ is the notation denoting a DCM that expresses a vector in the 'X' frame to the 'Y' frame and is a function of three angles (analogous to Euler angles).

$(p\phi_i, p\theta_i, 0)$ are the pulse azimuth and elevation angles from the primary AL axis,

$(d\phi, d\theta, d\psi)$ are the orientation offsets between the AL and the IMU,

$(\phi_i, \theta_i, \psi_i)$ are the Euler angles of roll, pitch and heading,

$(L_i, \lambda_i, 0)$ are the latitude and longitude angles.

The geo-referenced coordinates are then expressed in a local-level (NED) frame.

$$\underline{X_i}^{n} = C_e^n(L_o, \lambda_o, 0)\cdot\left[\underline{X_i}^{e} - \underline{O}^{e}\right] \tag{4}$$

where,

$\underline{X_i}^{n}$ is the i^{th} footprint position vector expressed in an NED frame whose origin is at latitude (L_o) and longitude (λ_o),

$\underline{O}^{e}$ is the position vector of the origin in ECEF frame.

3.2 INS DRIFT ESTIMATION

The INS position drift error introduced in the time interval between scanning of both the map (from forward pointing ALS) and the navigation terrain models (from aft-pointing ALS) is determined by matching both terrain models and observing the difference in their coordinates. Map-matching is done by a direct comparison of the terrain model height profiles using an appropriate metric for a discrete set of 3D position offsets within a predetermined 3D position search space.

The terrain models created by airborne scanning lasers are in the form of a point-cloud and, hence, point-cloud interpolation techniques must be devised such as the triangulation based scheme [9] given as:

$$h_{interp} = \frac{h_1A_1 + h_2A_2 + h_3A_3}{A_1 + A_2 + A_3} \tag{5}$$

where h_i are the heights of the vertices and A_i are the areas of the smaller triangles opposite to the vertices for $i = 1,2,3$. The horizontal coordinates of the aft terrain model are used to extract the heights from the reference map, using equation (5). Then, both sets of heights are compared for various position offsets $\delta\underline{x}$ using a normalized comparison metric, specifically, the Error Variance (EV) [5].

$$EV(\delta\underline{x}) = \frac{1}{N}\sum_{i=1}^{N}\left[(g_i(\delta\underline{x}) - h_i)^2\right] - h_{mean}^2 \tag{6}$$

where:

g_i is the i^{th} interpolated height,

h_i is the i^{th} geo-referenced height,

N is the number of points (out of the total points contained in the aft model) that have had valid circumscribing map triangles and a successful height lookup,

$$h_{mean} = \frac{1}{N}\sum_{i=1}^{N}(g_i(\delta\underline{x}) - h_i) \tag{7}$$

is the average difference between the two height profiles.

3.3 POSITION UPDATE

The IMU drift between both fore and aft terrain models at the j^{th} algorithm update is computed as:

$$\underline{\delta v}_j = \underline{\delta x}_j / \delta t_j \tag{8}$$

where:

$\underline{\delta v}_j$ is the IMU drift (ms^{-1}) in mission frame,

$\underline{\delta x}_j$ is the offset vector between both terrain models determined by the grid search, in mission frame,

δt_j is the time interval between the terrain models.

The updated IMU position error vector at time t_j is computed using the kinematics equation:

$$\Delta \underline{X}_j = \Delta \underline{X}_{j-1} + \underline{\delta v}_j \Delta t_{rj} \quad (9)$$

where Δt_{rj} is the time elapsed since the last position update ($\Delta t_{rj} = t_j - t_r$). Finally, the position update is formed as:

$$\underline{X}_{DALS\,j} = \underline{X}_{IMU\,j} + \Delta \underline{X}_j \quad (10)$$

where:

$\underline{X}_{DALS\,j}$ is the aircraft position computed by the DALS aiding algorithm at the time of j^{th} update,

$\underline{X}_{IMU\,j}$ is the aircraft position provided by the IMU at the time of j^{th} update.

4. FLIGHT TEST SETUP

On September 19, 2007, we embarked on a data collection effort on Ohio University's DC-3 flying laboratory. The Douglas DC-3 is a fixed-wing twin propeller driven aircraft and the one currently owned by Ohio University (call sign N7AP, pictured in Fig. 3) is equipped with some of the most modern avionics and navigation systems. Among other things, specific to this research mission, it is equipped with a Honeywell navigation grade INS (HG1150), Northrop Grumman tactical grade IMU (LN200), a RIEGL medium range ALS (LMS-Q280i), a RIEGL short range ALS (LMS-Q140i-80HR), and two NovAtel OEM4 GPS receivers, the antennas of which are mounted on the aircraft fuselage along the center-line. More information on each of the hardware/sensors is provided in the next sub-section.

4.1 HARDWARE DESCRIPTION

4.1.1 Honeywell HG1150 Navigation Grade INS

The INS provided the positions and attitude used in ALS footprint geo-referencing. It consists of ring laser gyros (RLG) for angular measurements. The attitude from the INS was treated as accurate (specifically the roll and pitch angles, the heading does have some drift as discussed later). Position accuracy typically showed 1 nmi/hr drift performance. The device interfaces through ARINC 429 and the 'ARINC words' of position coordinates i.e., latitude, longitude and altitude were unusable due to quantization. Hence, the position was derived by integrating the velocity outputs, which proved to be quite adequate.

Figure 3. The Douglas DC-3 aircraft was used to fly the research mission.

4.1.2 RIEGL LMS-Q280i Medium Range ALS

The LMS-Q280i is a medium range, pulsed ALS operating in the near infrared frequency, designated as Class 1 for eye-safe operation. The laser beam is deflected using a polygonal rotating mirror that provides the scanning mechanism. By mounting the device such that it scans along the lateral axis of the aircraft, we can get maximum coverage of the terrain below. Some technical specifications are provided in Table I [10][11].

4.1.3 RIEGL LMS-Q140i Short Range ALS

A generation older than the LMS-Q280i, the LMS-Q140i is a short range (~ 450 m) ALS that is also classified eye-safe and uses a polygonal rotating mirror to provide the scanning motion. Due to slightly different mechanical and optical assembly, the Q140 provides only half the

TABLE I. DUAL ALS OPERATIONAL PARAMETERS

Scan Parameter	Fore ALS	Aft ALS
Scan Rate	30 scans/sec	30 scans/sec
Scan Range (Field of View)	45°	60°
Pulse Repetition Rate (PRR)	24KHz	24KHz
Number of Mirror Facets	4	3
Scan Type	Linear, Unidirectional	Linear, Unidirectional
Pointing Angle from Nadir	30° Forward looking	0° Downward looking
Max. Range	1500 m	450 m

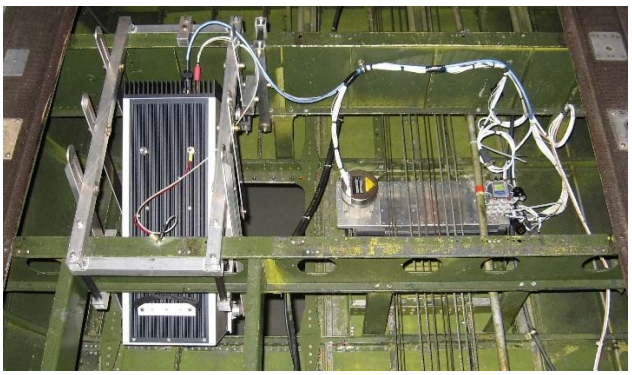

Figure 4. Dual ALS installation on the DC-3 aircraft.

pulse density as the Q280 and the device also has to be mounted differently to provide the same lateral scanning motion. A picture of the sensor installations below the aircraft floorboards is shown in Fig. 4.

4.1.4 NovAtel OEM4 GPS Receiver

A Wide Area Augmentation System (WAAS) enabled GPS receiver was used to collect pseudo-range, carrier phase, ephemeris and timing data to be used in post-processing and formation of the truth trajectory. The NovAtel receiver logs were processed with Waypoint Grafnav, a commercially available kinematic processing software. This truth trajectory is used for comparison of system accuracies. Two GPS antennas mounted on the aircraft fuselage along its center line and their receiver logs were also used for precise heading determination.

The one pulse-per-second (PPS) signal from one of the GPS receivers was used to calibrate the data-collection computer's processor clock that was used for time-tagging each of the sensor measurements. At this juncture, it may be useful to understand the different rates at which each of the sensor measurements come in, as provided in Table II.

TABLE II. SENSOR MEASUREMENT RATES

SENSOR OR SENSOR PARAMETER	MEASUREMENT RATE
Fore ALS	12000 Hz
Aft ALS	6000 Hz
INS roll and pitch	50 Hz
INS heading	25 Hz
INS velocity, position (integrated velocity)	10 Hz
GPS ("truth" after post-processing)	1 Hz
DALS/INS algorithm update	(1/3) Hz

4.2 SOFTWARE DESCRIPTION

The data collection computer ran on QNX 6.3 Neutrino real-time operating system (RTOS). Each of the sensors, i.e. INS, both ALS and the GPS receiver interfaced with the data collection computer through their dedicated device drivers written in 'C' programming language. Using the PPS signal each device driver time-tagged its respective sensor measurement. A data recording program, also written in C, interacted with each of these sensor device drivers to read data and write to a file on the hard disk. All other processing was done off-line, post flight.

4.3 FLIGHT TEST LOCATION

The flight test was conducted over Ohio University's Airport (KUNI) in Albany, OH and the main campus in Athens, OH. A plot of the truth trajectory is shown in Fig. 5. We took off at KUNI and performed two approached before proceeding on towards the University campus in Athens where we performed three circular loops. After that we returned to KUNI, performed a few more circular flights (for a different research mission) before finally landing. The portion of flight data used for the analyses and results presented here is highlighted in green.

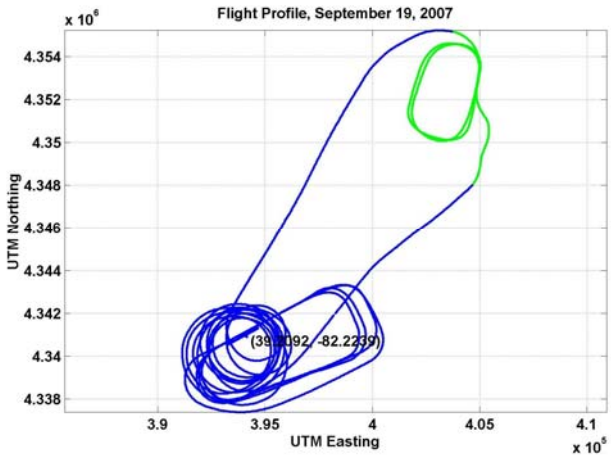

Figure 5. Flight Test Profile.

5. CHALLENGES OF DATA PROCESSING

Many real-world challenges that are usually conveniently ignored while performing simulations present themselves with renewed importance when working with real data. This section is focused towards some of those challenges.

5.1 VEGETATION

The existence of trees in geo-referenced ALS data introduces a large amount of noise-like error in the height dimension. This error adversely affects the correlation of fore and aft terrain maps by distorting the surface of EV comparison metric of equation (6). The distorted EV surface leads to false minima and thus incorrect offsets between the two maps. This in turn means that the DALS aiding algorithm cannot estimate the INS velocity and position errors correctly, leading to degraded performance. A plot of overlapping fore and aft ALS terrain maps, in the presence of vegetation is shown in Fig. 6. On comparison with Fig. 1, we can see how much

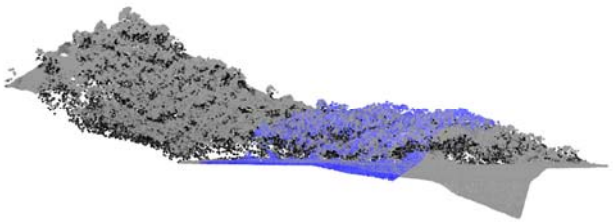

Figure 6. Presence of Vegetation in the ALS Maps.

Figure 7. Dense and sparse vegetation at the flight test location.

off the real data is from the synthesized! In anticipation of the vegetation effects, both ALS were programmed before the flight test to record the last return of each pulse. (They can record either the first return or the last return.) In spite of this, in dense vegetation conditions, the last return can still come from the treetops. The high noise is contributed by the fact that the laser pulses penetrate through different levels of the trees; reflecting from the tree-tops, branches and some from the ground. An illustrative picture of the extent of trees that were present at the flight test location is shown in Fig. 7.

A number of possible solutions can be sought to overcome the effects of vegetation, such as:

- Algorithms for spatial filtering and tree-removal [12].
- Estimation of bare-Earth terrain model from sparse laser returns.
- Use of better ALS sensors, such as a full waveform digitizing laser [13] that can record multiple returns from various levels of penetrations. The last return of sufficient energy will probably be a ground return.

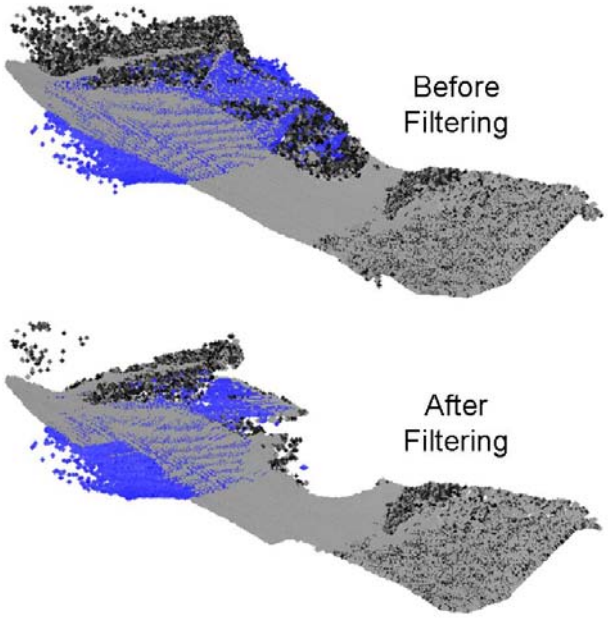

Figure 8. Demonstration of tree removal by filtering.

For our purpose here, we designed a simple spatial filter for tree-removal, the results from which are shown in Fig. 8. As can be seen, the filter removes most points that are trees with some residuals, and is reserved for further improvements.

5.2 LEVER ARM AND ORIENTATION OFFSET

The lever arm $\left(\underline{L}^{b}_{INS\to AL}\right)$ and angular orientation offset $(d\phi, d\theta, d\psi)$ that invariably exists between each ALS and the INS figure prominently in the laser pulse footprint geo-referencing equations, as given by equation (2).

$$\underline{\chi_i}^{\,b} = \underline{L}^{b}_{INS\to AL} + C^{b}_{AL}(d\phi, d\theta, d\psi)\cdot \underline{\chi_i}^{\,AL} \qquad \text{Copy of (2)}$$

An illustration of the lever arm and orientation errors between ALS and INS frames is shown in Fig. 9.

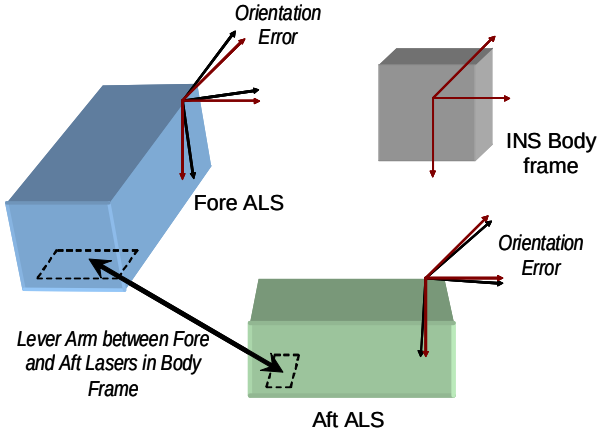

Figure 9. Illustration of Lever Arm and Orientation Offsets.

Accounting for these offsets is the first step in geo-referencing and any errors in computing these offsets propagate non-linearly through the rest of the geo-referencing process. Especially detrimental are the orientation offsets that contribute to large footprint errors. The position error, caused due to the orientation offset is a function of range $\delta\underline{l} = r\cdot\delta\underline{\Theta}$ and hence each point of the map is affected differently, thus making it difficult to apply any simple correction to the final map as a whole.

5.3 INS HEADING ERROR

We considered the attitude output of the navigation grade INS as perfect with very little noise. This is a reasonable assumption for the roll and pitch angle outputs but even navigation grade gyroscopes are limited in their ability to measure the earth rate. As a result, the heading alignment is biased and the measurements drift slowly over time. Preliminary analysis of the effect of an initial INS heading error was published in [7] and re-iterated here. The error vector due to the heading bias, defined from the

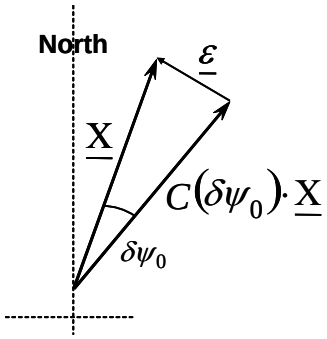

Figure 10. Heading bias and the resulting error vector.

erroneous position to the true position, is illustrated in the graphic of Fig. 10. The error in the horizontal coordinates of the DALS/INS solution can be expressed in terms of the heading bias $\delta\psi_0$ and the estimated displacement vector $\underline{\tilde{X}}$ as:

$$\begin{aligned}\underline{\varepsilon} &= C^T(\delta\psi_0)\cdot\underline{\tilde{X}} - \underline{\tilde{X}} \\ &= \left[C^T(\delta\psi_0) - I\right]\cdot\underline{\tilde{X}}\end{aligned} \tag{11}$$

Writing equation (11) in matrix form and applying small angle approximations yields:

$$\begin{bmatrix}\varepsilon_x \\ \varepsilon_y\end{bmatrix} = \begin{bmatrix}0 & -\delta\psi_0 \\ \delta\psi_0 & 0\end{bmatrix}\cdot\begin{bmatrix}\tilde{x} \\ \tilde{y}\end{bmatrix} \tag{12}$$

If the horizontal error is independent of all other error sources, then equation (12) allows us to estimate the heading bias error by knowing the horizontal error (on comparison with truth) and the displacement from initial position.

6. DALS/INS RESULTS

INS corrections were computed and applied using the DALS aiding algorithm, formulated previously and the results are shown in this section. Fig. 11 shows the error in North, East and the total horizontal error is shown in Fig. 12. The algorithm achieved a horizontal drift of 5m in 8 minutes for the flight segment under consideration. Although at the end of 8 minutes the DALS/INS error is small, the out-of-phase sinusoid on the north and east error suggests there is residual heading error left over after calibration and there is potential for improvement. A portion of that error may also be caused due to vegetation. The vertical error (Fig. 13), on the other hand, ramps away drastically which can be attributed to vegetation effects in the data. Filtering off the trees and applying the DALS/INS algorithm on relatively clean ALS map data improves the vertical error performance significantly.

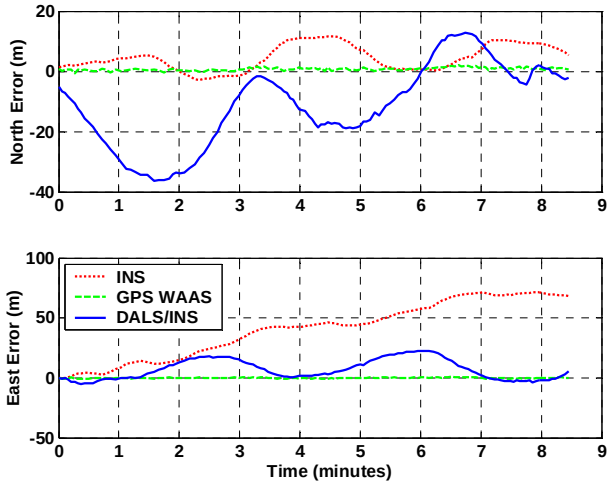

Figure 11. North and East direction errors.

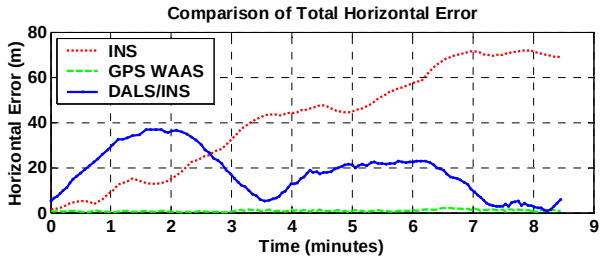

Figure 12. Horizontal Error.

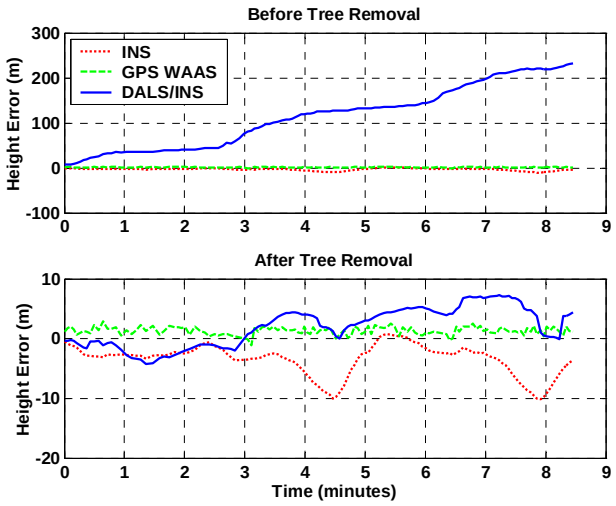

Figure 13. Height error before and after tree removal.

7. CONCLUSIONS AND FUTURE WORK

DALS/INS integration results are demonstrated as proof-of-concept using flight test data. The integrated system has the potential to provide improved autonomous navigation performance for extended periods of time in non-GPS and unknown terrain environments. The proposed system uses aircraft-autonomous sensors; namely, the INS, two ALS sensors and a timing reference.

Similar to inertial navigation, this system is also dead reckoning in nature and computes relative position changes from one epoch to the next. The integrated solution is a random walk process as seen from previous analyses and further results are needed for a quantitative measure of its drift performance. Such a system could ensure mission continuity during temporary GPS outages. As optical sensors continue to reduce in size and cost, this system may become feasible for inhabited and uninhabited aerial vehicle navigation in the near future.

The algorithm presented here has the potential for improvement by the formulation of a Kalman filter for integration as well as improved filtering of ALS measurements to eliminate environment noise and thorough calibration of systematic errors.

8. ACKNOWLEDGMENTS

This research and flight testing was sponsored by the Northrop Grumman Corporation (NGC). Particular thanks to Phil Bruner of NGC for his support. Thanks to Jim van Rens of RIEGL Laser Measurement Systems for his advice regarding installation of the laser scanners. Thanks to the Air Force Research Labs (AFRL), Dayton, OH for supporting this project and also to Honeywell, Inc. for the use of their HG1150 INS. We are thankful to Jay Clark, chief of mobile labs and Paul Nilles for sensor installation and aircraft certification and the DC-3 pilots Bryan Branham and Dr. Richard McFarland for the flight test.

9. REFERENCES

[1] John A. Volpe National Transportation Systems Center, "Vulnerability Assessment of the Transportation Infrastructure Relying on the Global Positioning System", Final Report, August 29, 2001.

[2] Baird, C. A. and M. R. Abramson, "A Comparison of Several Digital Map-Aided Navigation Techniques", *Proceedings of the IEEE PLANS*, pp. 286-293, 1984.

[3] Hostetler, L. D., R. C. Beckman, "The Sandia Inertial Terrain Aided Navigation System", Sandia Laboratories, Albuquerque, NM, SAND77-0521, 1977.

[4] Campbell, J., M. Uijt de Haag and F. van Graas, "Terrain-Referenced Precision Approach Guidance: Proof-of-Concept Flight Test Results", NAVIGATION Journal of the Institute of Navigation, Vol. 54, No. 1, pp. 21-29, 2007.

[5] Vadlamani, A. K. and M. Uijt de Haag, "Use of Laser Range Scanners for Precise Navigation in Unknown Environments", in *Proceedings of the ION GNSS 19th International Technical Meeting of the Satellite Division*, Fort Worth, TX, 2006, pp. 1104-1114.

[6] Vadlamani, A. K., and M. Uijt de Haag, "Aerial Vehicle Navigation Over Unknown Terrain Environments Using Inertial Measurements and Dual Airborne Laser Scanners or Flash LADAR", in Proceedings of SPIE vol. 6550, Laser Radar Technology and Applications XII, Turner and Kamerman, eds.

[7] Vadlamani, A. K. and M. Uijt de Haag, "Sensor Data Analysis for a Dual Airborne Laser Scanner Aided Inertial Navigator", in *Proceedings of the ION 63rd Annual Meeting*, Cambridge, Massachusetts, 2007, pp. 89-96.

[8] Titterton, D. H. and J. L. Weston, "*Strapdown Inertial Navigation Technology*", Peter Peregrinus Ltd., 1997.

[9] Amidror, I., "Scattered Data Interpolation Methods for Electronic Imaging Systems: A Survey", *SPIE and IS&T Journal of Electronic Imaging*, vol. 11, issue 2, pp. 157-176, April 2002.

[10] Riegl Laser Measurement Systems, LMS-Q280i Airborne Laser Scanner, Technical Documentation and Users Instructions, 2004.

[11] Riegl Laser Measurement Systems, LMS-Q140–60HR, Technical Documentation and User's Instructions, 2001.

[12] Sithole, G. and G. Vosselman, "Report: ISPRS Comparison of Filters", International Society of Photogrammetry and Rmoete Sensing (ISPRS), Commission III, Working Group 3, August 2003.

[13] Riegl Laser Measurement Systems, LMS-Q560 Datasheet, dated 15Jan2008, accessed from http://www.riegl.com/.